Materials Research. 2013; 16(4): 772-778
DOI: 10.1590/S1516-14392013005000047

Normalizing Effect on Fatigue Crack Propagation at the Heat-affected Zone of AISI 4140 Steel Shielded Metal Arc Weldings

***B. Vargas-Arista*[a]*, J. Teran-Guillen*[b], *J. Solis*[a], *G. García-Cerecero*[c], *M. Martínez-Madrid*[b]**

[a]*División de Estudios de Posgrado e Investigación – DEPI, Instituto Tecnológico de Tlalnepantla – ITTLA, Av. Instituto Tecnológico, s/n, Col. La Comunidad, Tlalnepantla de Baz, CP 54070, Estado de México, México*
[b]*Instituto Mexicano del Transporte, Coordinación de Ingeniería Vehicular e Integridad Estructural – CIVIE, Km 12+000 Carretera Qro.-Galindo Sanfandila, Pedro Escobedo, CP 76700, Qro. México*
[c]*Posgrado en Tecnología de la Soldadura Industrial, Corporación Mexicana de Investigación en Materiales – COMIMSA, Ciencia y Tecnología, 790, Col. Saltillo 400, Saltillo, CP 25290, Coahuila, México*

Received: March 5, 2012; Revised: December 19, 2012

The fractography and mechanical behaviour of fatigue crack propagation in the heat-affected zone (HAZ) of AISI 4140 steel welded using the shielded metal arc process was analysed. Different austenitic grain size was obtained by normalizing performed at 1200 °C for 5 and 10 hours after welding. Three point bending fatigue tests on pre-cracked specimens along the HAZ revealed that coarse grains promoted an increase in fatigue crack growth rate, hence causing a reduction in both fracture toughness and critical crack length, and a transgranular brittle final fracture with an area fraction of dimple zones connecting cleavage facets. A fractographic analysis proved that as the normalizing time increased the crack length decreased. The increase in the river patterns on the fatigue crack propagation in zone II was also evidenced and final brittle fracture because of transgranular quasicleavage was observed. Larger grains induced a deterioration of the fatigue resistance of the HAZ.

Keywords: *heat affected zone, fatigue, SMAW process, 4140 steel*

1. Introduction

The lifetime of a component or structure under cyclical, alternating, repetitive or fluctuating loads is frequently considered to be determined by the crack initiation site, crack propagation and the final catastrophic fracture, which are allwell-identified stages of fatigue damage, as the core mechanism of degradation and failure in structural components[1]. These stages are particularly affected by the grain size, an important engineering parameter that controls mechanical properties in materials, such as yield strength[2]. Vehicular bridges that work under cyclical loads and have welded joints in their most critical components as the braces are a case in point. Structures are said to be functionally static, in bridges for instance, which have the particular function of maintaining a static connection between shorelines. These structures encompass manufactured components such as beams, tubes, plates, and sections, all of them mainly joined by welding and bolting. Service conditions involving traffic loads, collisions, temperature changes or even gusts of wind induce both static functional and cyclical loads on bridges.

The evaluation used for the crack propagation rate in order to predict residual life is the fatigue methodology applied to structures for design purposes[3]. In practice, when the construction of bridges is planned, an important factor that has to be taken into account is the fatigue behaviour of the potential materials to be selected like the cast steel and alloy steel. In particular, the AISI 4140 chrome and molybdenum low alloy steel, with limited weldability and moderate hardening as a function of the grain size, could be proposed in the manufacturing of braces of bridges. This steel can be joined using shielded metal arc welding (SMAW). A key outcome of this welding process is the generation of a HAZ, which is formed by several heterogeneous recrystallized microstructures classified as coarse and fine grained HAZ. The formation of these complex microstructures becomes even more severe for joints using various welding beads by means of multi-pass arc welding resulting in the re-heating of the HAZ with critical mechanical properties[4].

Fatigue crack growth mechanisms in steel have received considerable attention in the quest to understand the principal variables affecting this stage of the fatigue failure process in order to improve the integrity of metallic components and structures[5]. One case is the fatigue properties in the multi-pass heat-affected zone (HAZ) of 800 MPa grade high performance steel, which is commonly used in bridges and buildings. The fatigue crack growth rate of intercritically reheated coarse-grained HAZ (ICCG-HAZ) was the fastest among local zones as the coarse and fine-grained, due

*e-mail: bvarista26@yahoo.com.mx

to rapid crack initiation and propagation via the massive martensite–austenite constituent[6]. A second case is the fatigue crack growth behavior of welded 4130 steel. The d*a*/d*N* value in the HAZ was higher than that in the as-quenched base metal plate resulting in more severe intergranular fracture and tempered martensite embrittlement[7].

A third case is the simulated coarse-grained HAZ with LT orientation for welded high strength low alloy steel, which shows a remarkable decrease in fracture toughness with an increase in the size of the austenite grain and the volume fraction of martensite/austenite constituent distributed in the shape of a network[8]. Another example is the effect of normalizing at 1200 °C during 5 and 10 hours on the grain size and Vickers hardness of weldments by shielding metal arc welding of AISI 4140 steel. For the HAZ normalized at 5 hours, the microstructure showed idiomorphic and acicular ferrite. However, at 10 hours the grain size radically increased resulting in grain growth and microhardness values decreased (12%) with the increment in the time, which was related to the allotriomorphic ferrite on large austenitic grains containing acicular ferrite[9].

Additionally, the investigation of degradation of fracture toughness for the ICCG-HAZ in welded SN490 structural steel is reported. The cracks in this HAZ, with the worst toughness, were found to initiate at the intersection of bainitic ferrite followed by propagation in cleavage resulting in the brittle fracture initiation mechanism. In some crack propagation regions, adjacent cleavage facets are connected by shearing, thus producing dimple zones[10]. Moreover, there is a study of high cycle fatigue properties of welded joints on quenched and tempered AISI 4340 steel which was manufactured using the SMAW process and different steel welding consumables. The joints made using low hydrogen ferritic AWS E11018-M steel electrodes showed superior fatigue resistance when compared to other joints. An increase of 13% in fatigue life has been recorded in these joints, which was then linked to the larger yield strength and microstructure of acicular ferrite in the weld metal region[11]. However, fewer contributions have been published on the fractography of fatigue crack propagation behaviour in the HAZ on low-alloy steels such as AISI 4140. This work focuses on the mechanical and fractographic analysis of the fatigue crack propagation at the HAZ normalized with different grain sizes in welded joints of the aforementioned steel. The justification of this work is based on the fact that the HAZ is a deleterious microstructural zone of lower toughness where fatigue initiation sites are nucleated in welded joints.

2. Experimental Procedure

2.1. *Test material and welding procedure*

150 × 300 × 25.4 mm plates of AISI 4140 steel were joined using manual shielded metal arc welding (SMAW) performing several-passes through a double bevelled configuration at 45° (Figure 1a) with an AWS E7018 filler metal. An AWS D1.1 pre-qualified welding procedure specification (WPS)[12] was followed to weld the plates of the steel[9]. Table 1 shows the chemical composition of the base metal and filler metal given for the as-received condition, complying with specifications AISI 4140[13] and AWS A5.5[14] respectively.

The mechanical properties reported by the supplier for the base and filler metals in the as-received condition are registered on Table 2. These values also complied the mentioned standards[13,14]. The proposed welded joint with a lower mechanical resistance than the specified design was fabricated because the base metal showed a higher resistance than the filler metal. This welded joint was established to reduce the resistance of the steel[15].

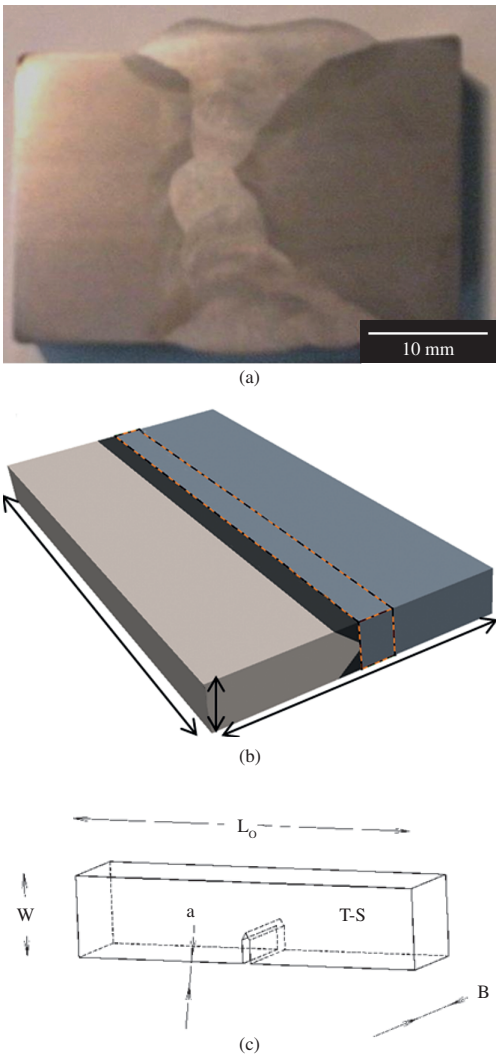

Figure 1. (a) welded joint obtained by the SMAW process, (b) schematic representation of the welded plates, and (c) fatigue specimen used in this study.

Table 1. Chemical composition of the base and filler metals (in wt. (%)).

Material	Element (wt. (%))							
	C	Mn	Si	Cr	Mo	P	S	C.E.
4140 steel	0.43	0.82	0.22	0.88	0.20	0.006	0.004	0.85
AWS 7018	0.05	1.30	0.30	–	–	–	–	0.26

Table 2. Mechanical Properties of the AISI 4140 steel and AWS E7018 filler metal.

Material	Hardness	Yield strength (MPa)	Tensile strength (MPa)
AWS E7018	79 HRB	437	485
4140 steel	30 HRC	675	1020

2.2. *Fatigue test*

Fatigue pre-cracked specimens for three-point bending were machined from the welded joints (Figure 1b) so that they could be used in the fatigue crack propagation tests, using length L = 80 mm, width W = 18 mm and thickness B = 18 mm (Figure 1c) in accordance with ASTME-399[16]. A stress concentrating notch was made along the HAZ that allowed the specimen to be pre-cracked up to an initial length (a_O) of 7.8 mm in the long transverse – short transverse (T-S) orientation of the plate. The specimens were normalized at 1200 °C for 5 and 10 hours and afterward were air-cooled. No statistical analysis was performed due to the fact that there was insufficient material available to machine fatigue specimens for each normalized condition.

A servo-hydraulic machine, Instron model 8801 with a 100 kN load cell, a three-point bending device and da/dN program were used for the fatigue crack propagation tests. The f(a/w) dimensionless geometrical factor[16] was calculated using Equation 1, taking the length of the notch as the a_0 value and measuring the width of the specimen, W.

$$f\left(\frac{a}{W}\right)=3\sqrt{\frac{a}{W}}\cdot\frac{1.99-\left(\frac{a}{W}\right)\left(1-\frac{a}{W}\right)\left[2.15-3.93\frac{a}{W}+2.7\left(\frac{a}{W}\right)^2\right]}{2\left(1+2\frac{a}{W}\right)\left(1-\frac{a}{W}\right)^{3/2}} \quad (1)$$

where: a = Crack size, mm; W = Specimen width, mm.

Initiating with a value of 15 MPa $m^{1/2}$ and R = 0.1, both $P_{máx} = \Delta P/(1-R)$ and $P_{mín} = 0.1P_{máx}$ were determined. Since ΔP was constant during the test, ΔK increased as the crack grew and was calculated by the program. Equation 2 was used to calculate the stress intensity factor (K)[16] in MPa $m^{1/2}$.

$$K=\frac{PS}{BW^{3/2}}\cdot f\left(\frac{a}{W}\right) \quad (2)$$

where: P = Force, N; B = Specimen thickness, mm; S = 4W ± 0.2W = Distance between the support rollers, mm; W= Specimen width, mm; a = Crack length, mm.

A 5× magnification stereoscope was used to follow the crack propagation using as reference a set of marks which were made every 0.25 mm on the side surface of the specimens from the tip of the notch using a height Vernier. This procedure was performed in order to allow for the estimation of the error between the experimental measurements of the crack length and those obtained with the software. Sigmoidal crack propagation curves (da/dN) were acquired as a function of ΔK. There was a lineal behaviour in the crack growth curve in region II, which was described by the Paris relationship[1].

$$\frac{da}{dN}=C(\Delta K)^m \quad (3)$$

where: a = Crack length, mm; N = Number of cycles; C and m = Material constants.

2.3. *Fractography*

After the fatigue tests, the fractographical analysis of the fracture surfaces along the normalized HAZ of welded AISI 4140 steel, obtained from the fatigue fractured specimens, was carried out using a JEOL JSM 6490 LV scanning electron microscope operated at 15 kV, with a secondary electron and working distance of 41 mm.

2.4. *Normalizing heat treatment*

Normalizing at high temperature of 1200 °C for 5 and 10 hours using a resistance furnace was performed on specimens to obtain notable and measurable growth of the grain size[17], which was limited by the moderate hardenability due to the chemical composition of the steel[13]. The specimens were subsequently removed from the furnace and air-cooled. This treatment was based on the fact that during the welding thermal cycles, the HAZ reached a temperature of approximately of 1200 °C[8], thus resulting in the growth of grains that can be modified for long periods of time, for hours. The normalizing changed the grain size which then has a strong influence on the tensile properties of the HAZ, mainly the yield strength. However, there was insufficient material available to directly determine the yield strength of all the specimens as a function of grain size. Therefore, this mechanical property was calculated by the Hall-Petch Equation 4[17]. This parameter permits a good estimate of the yield strength as a function of grain size.

$$\sigma_{ys}=\sigma_o+k_d\,d^{-½} \quad (4)$$

where: σ_{ys} = Yield strength, MPa; σ_o = Yield strength of the as-received condition, 675 MPa for this study; k_d = Constant of material, 0.112 for this study determined by the slope plotted of K_{Ic} vs $d^{-½}$; $d^{-½}$ = Average grain diameter, m.

The resulting values of the yield strength for the HAZ normalized at 1200 °C are shown in Table 3. There was a considerable decrease in strength as the grain size increased[17]. This relationship could be correlated with the reduction of Vickers hardness during grain growth which is reported elsewhere[9].

Table 3. Yield strength calculated for the HAZ normalized at 1200 °C with different grain size.

Condition	Grain size (μm)	Yield strength (MPa)
As-received	10	710
Normalized at 5 hours	55	690
Normalized at 10 hours	230	682

3. Results and Discussion

3.1. *Fatigue crack propagation*

The fatigue crack propagation tests provided the propagation rate (da/dN) as a function of the amplitude of the stress intensity factor (ΔK) at the HAZ for specimens normalized at 1200 °C for 5 and 10 hours and as-received condition. The effect of the increase in the austenitic grain size induced by the normalizing treatment on the fatigue behaviour was promotion of the fatigue crack propagation which brought a decrease in the critical crack size and fracture toughness with the consequent increase of the values of the *m* exponent (slope of the stage II of curve described by the Paris regime, i.e., where the linear elastic fracture mechanics become dominant). After normalizing for 10 hours, the *m* exponent showed a 119% increase when compared to the as-received condition.

The increase in grain size shifted the curve to the left, which shows an increase in fatigue crack growth, as shown in Figure 2. The normalized specimen for 10 hours and final grain size of 230 μm presented the highest crack propagation rate, i.e., the lowest fatigue resistance. When the curves of the different conditions were compared, a larger dispersion with higher values of ΔK was found, which indicated that there was great influence in the heterogeneous microstructures of the HAZ. A greater resistance to fatigue crack propagation was found in specimens without normalizing treatment.

The fatigue crack growth rate as a function of the grain size in the HAZ, induced by the normalizing heat treatment, is illustrated in Figure 3. An increase in the fatigue crack propagation is clearly evident with the increase in the grain size, which relates back to the lower interactions between the actual crack and the reduced length of grain boundaries, resulting in minor obstacles and intersections during crack propagation along the heterogeneous microstructures in the HAZ that were thermally affected by the normalizing process[9].

The increase in grain size causes reduction in the number of grains and a decrease in the surface area of grain boundaries could be related to the disappearance of small grains into the large grains. Any dislocation within the grain must move a great distance to encounter a grain boundary and stop. Therefore, the increase in grain size generated a decrease in the yield strength[17] of the HAZ, as can be seen in Table 3, resulting in lower fatigue resistance.

A reduction of the critical crack length (a_c) was also observed with the increase of the grain size, as can be observed in Figure 4. There was a notable 39% decrease in the final crack length for the specimens normalized for 10 hours when compared to those of the as-received condition, indicating induced fatigue crack propagation. The decrease in a_c could be associated with the reduction in the yield strength as a consequence of the reduction in the number of grains, thus giving fewer grain boundaries that impede crack propagation. Therefore, the final fracture was favoured.

The effect of the grain size on the fracture toughness (K_{Ic}) at the HAZ of the normalized specimens is depicted in Figure 5. The behaviour shown is similar to that of the critical crack length mentioned earlier, which was due to the fact that the K_{Ic} factor is directly proportional to crack size as shown in Equation 2. The effect of the increase in grain size on fracture toughness was a drastic reduction in relation

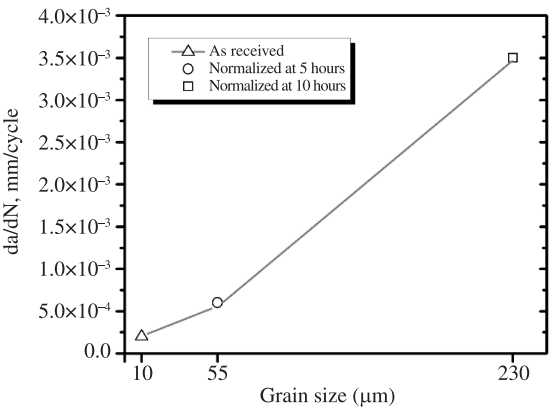

Figure 3. Plot of fatigue crack growth rate as a function of the grain size for the HAZ normalized at 1200 °C for different time periods.

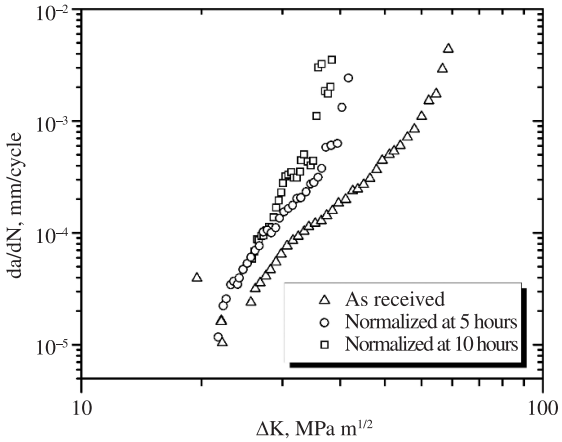

Figure 2. Plot of crack growth rate behaviour with the stress intensity factor for the HAZ normalized at 1200 °C for different time periods.

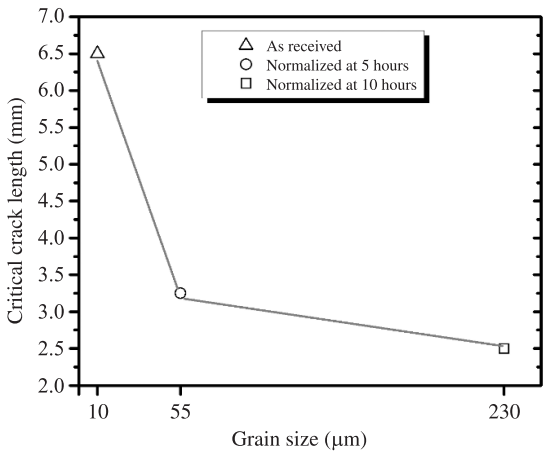

Figure 4. Plot of critical crack length as a function of grain size for the HAZ normalized at 1200 °C for different time periods.

to the minor area in grain boundaries. Similar toughness behaviour was reported for the high strength low alloy steel[8]. The specimens normalized for 10 hours showed a 56% decrease in K_{Ic} compared to those in as-received condition, a change that favoured crack growth and therefore reduced fatigue resistance.

3.2. *Fractography*

Fatigue behaviour involving the increase in fatigue crack growth, the reduction of the critical crack length and the decrease in fracture toughness were indirectly confirmed using a fractographic analysis of the fracture surfaces obtained from the fatigue fractured specimens for the HAZ normalized at 1200 °C for 5 and 10 hours. These surfaces are shown in Figure 6, where we can macroscopically see that there are not ramifications or scalings and fracture is perpendicular to the opening direction for each experimental condition. We can also observe the root notch (lowest area of the fractography of Figure 6a), the crack propagation in zone II with a flat surface and variable extension after the root notch (middle area of Figure 6b), and zone III shows a mixed (brittle and ductile) final fracture (upper area of Figure 6c).

The greatest crack extension appeared on the fractured surface of the as-received specimen (Figure 6a), followed by a ductile fracture area with rough appearance[17]. The specimens normalized for 5 hours showed a flat surface and a decrease of the crack growth zone length, followed by a zone III of brittle fracture with a noticeable bright and granular appearance (Figure 6b). Specimens normalized for 10 hours, in turn, had a fractured surface that evidenced the lowest crack propagation zone length, followed by a larger area of brittle fracture with secondary cracking (Figure 6c).

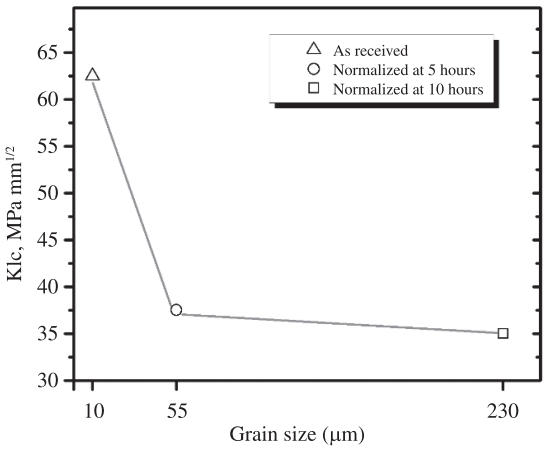

Figure 5. Plot of fracture toughness as a function of the grain size for the HAZ normalized at 1200 °C for different time periods.

There was a 77% decrease in zone II crack growth comparing specimens normalized for 10 hours to the as-received ones, showing that this fractured surface had the lowest crack propagation. In conclusion, the decrease of the critical crack length with the increase of the time used in the normalized process was confirmed, promoting the crack propagation under fatigue conditions with the consequent detriment of fatigue resistance.

SEM observations on the fractured surfaces revealed that the transgranular crack growth[5] in zone II showed a front parallel to the notch and well-defined river patterns in the direction of propagation which, in turn, presented a significant change in the appearance produced as a result of the increase in the normalizing time as shown in Figure 7. Crack propagation on the fractured surface of the as-received specimens exhibited a smaller amount of river patterns on the rough surface[17] with slightly plastic deformation (Figure 7a), whereas in the specimen normalized for 5 hours the amount of such river patterns increased on a lesser rough surface (Figure 7b).The greatest amount of river patterns appeared on a smooth surface for a specimen normalized for 10 hours, indicating the largest crack growth (Figure 7c). The aforementioned fracture features could be related to the decrease in the yield strength linked to the increase in average grain diameter.Therefore, the effect of the normalizing process on the fractured surfaces was a large production in the amount of river patterns along the surface with the increase in time, i.e., greater transgranular crack propagation.

The analysis of the final fracture in zone III showed, in the as-received specimen, a ductile fracture with long, fine dimple morphology in the direction of the crack propagation (Figure 8a). Moreover, the presence of large and thin non-metallic inclusions led to the formation of hollows along the matrix-inclusion interface. However, after normalizing treatment for different times at 1200 °C, a transgranular brittle fracture caused by quasicleavage with well-defined flat facets, river patterns in the propagation direction, secondary

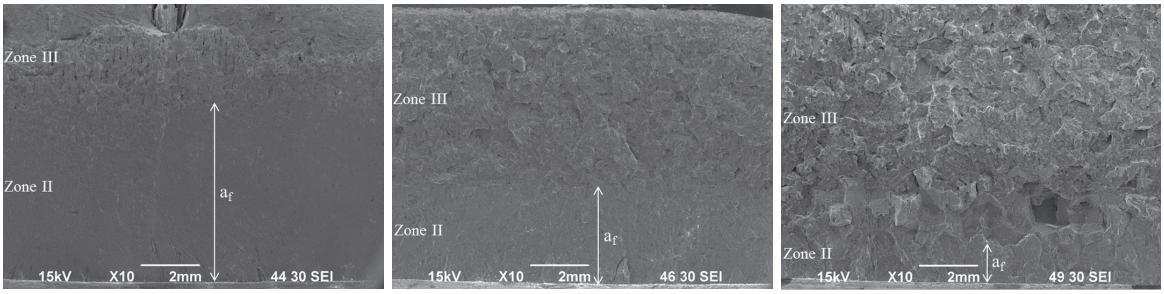

(a) (b) (c)

Figure 6. Fractography of fatigue fractured surfaces for HAZ specimens: (a) the highest critical crack size on the as-received condition, (b) normalized for 5 hours with lower crack size, and (c) normalized for 10 hours with the lowest crack size.

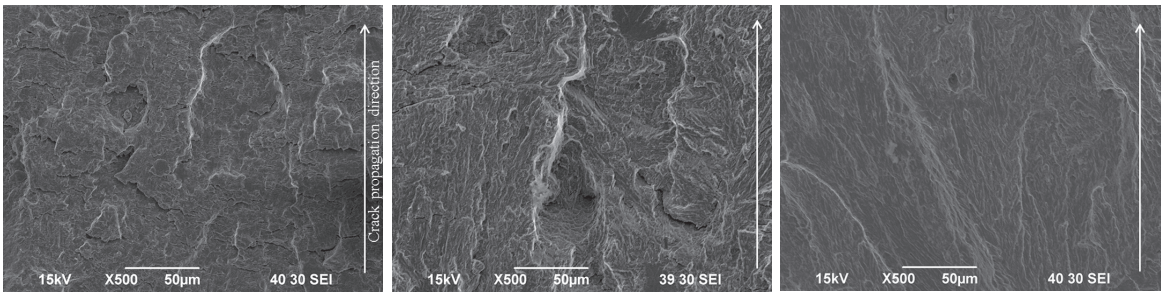

(a) (b) (c)

Figure 7. Fractography of fatigue fractured specimens for the HAZ at crack growth (Zone II): (a) the lowest amount of river patterns on the as-received condition, (b) normalized for 5 hours with increase in the amount of river patterns, and (c) normalized for 10 hours with the highest amount of defined river patterns.

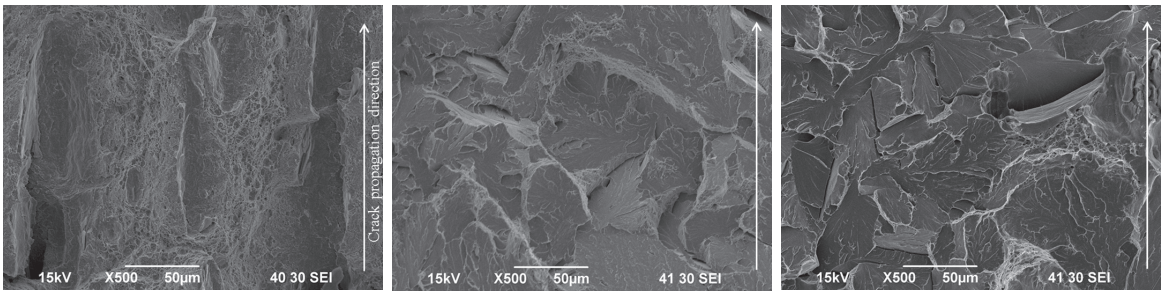

(a) (b) (c)

Figure 8. Fractography of fatigue fractured specimens for the HAZ at final fracture (Zone III): (a) dimple morphology and long thin hollows on the as-received condition, (b) normalized for 5 hours, and (c) normalized for 10 hours with brittle fracture showing defined cleavage facets and dimple network.

cracking and a dimple network over the adjacent cleavage facet boundaries[10] were revealed on the specimens normalized for 5 hours (Figure 8b) and 10 hours (Figure 8c). A remarkable increase of 133% of zone III extension in the final fracture surface of the specimen normalized for 10 hours was reached in comparison to the as-received condition. The fractographic features indicated that the normalizing process facilitated the fatigue crack propagation that gave way to transgranular brittle fracture along the HAZ.

3.3. *Summary*

In summary, the fatigue and toughness behaviour of the HAZ after normalizing at 1200 °C for different times was an original contribution due to the fact that this behaviour was different to the published findings for the steels as base metal[1,17]. Therefore, fatigue resistance decreased when normalizing treatment was applied due to the larger austenite grains produced in the HAZ specimens, i.e., the length of grain boundaries decreased, resulting in a deterioration of yield strength, which managed to accommodate more plastic deformation and flow stress generated ahead of the crack. The larger grains accumulated a high density of dislocations in active slip bands associated with the crack growth and the severity of the stress gradient at the notch. All this translated into faster growth rates and higher stress concentrations at the barriers, like the grain boundaries. Thus, the stress gradient and level of applied stress make it possible for the crack to overcome few grain boundaries with a massive plastic slip beyond each overcome barrier.

Moreover, there was transgranular crack growth[5] in zone II and a transgranular brittle quasicleavage fracture[10] in zone III as the size of austenite grain increased with the time spent in the normalizing process. When the specimen normalized for 10 hours was compared to the as-received condition, there was a 56% drop in the fracture toughness associated with the 39% decrease of critical crack length on zone II of the crack propagation, which in turn, shrunk 77% in extension. Furthermore, a 133% increase was found in the extension in zone III of the final fracture with crack propagation due to a brittle fracture caused by transgranular cleavage. This final fatigue fracture behaviour was linked to the degradation of yield strength and Vickers hardness[9] because of fewer grain boundaries.

4. Conclusions

The heat-affected zone (HAZ) of SMAW welded AISI 4140 steel specimens was susceptible to normalizing treatment at 1200 °C resulting in an increase of the size of austenite grain as a function of time, which induced a radical reduction in fatigue resistance, resulting in fatigue crack growth and brittle quasicleavage fracture, both through a transgranular mechanism.

The deterioration of fatigue resistance was linked to a reduction of yield strength as a consequence of a decrease in the over-all length of grain boundaries, producing less obstacles and intersections for crack propagation within the coarse grains of the modified microstructure of the HAZ.

Zone II of transgranular crack propagation presented a remarkable decreased in its extension according to the normalizing time. This later was associated with the increase in the well-defined river patterns throughout the fracture surface and a reduction of the fracture toughness as well as critical crack length.

The increase in grain size caused a transgranular brittle fracture in zone III of the final fracture, which was associated with the presence of well-defined flat facets of cleavage and a dimple network over the adjacent cleavage facet boundaries.

Acknowledgements

The authors wish to thank the experimental and financial supports received from the Corporación Mexicana de Investigación en Materiales (COMIMSA).

References

1. Schijve J. *Fatigue of structures and materials*. Kluwer Academic Publishers; 2004.
2. Courtney HT. *Mechanical Behavior of Materials*. 2. ed. McGraw Hill; 2000.
3. Pemov I, Murozov Y, Mulko G and Shafigin E. Improving the range of grades of steel for bridge construction. *Metalurgist*. 2000; 44(1):87-95.
4. González-Gutiérrez S, Vargas-Arista B, Solís J and García-Vazquez F. Efecto de la velocidad de alimentación sobre la microestructura y dureza en uniones soldadas multipasos por proceso GMAW en acero ASTM A633. In: *Proceedings of the 32th Congreso Internacional de Metalurgia y Materiales*; 2010; Saltillo, México. Saltillo: Instituto Tecnológico de Saltillo; 2010. p. 1-11.
5. Sadananda K and Vasudevan KA. Fatigue crack grow mechanisms in steels. *International Journal of Fatigue*. 2003; 25:899-914. http://dx.doi.org/10.1016/S0142-1123(03)00128-2
6. Sanghoon K, Donghwan K, Tae WK, Jong KL and Chang HL. Fatigue crack growth behavior of the simulated HAZ of 800 MPa grade high performance steel. *Materials Science and Engineering A*. 2011; 528(6):2331-2338. http://dx.doi.org/10.1016/j.msea.2010.11.089
7. Tsay WL, Li MY, Chen C and Cheng WS. Mechanical properties and fatigue crack growth rate of laser-welded 4130 steel. *International Journal of Fatigue*. 1992; 14(4):239-247. http://dx.doi.org/10.1016/0142-1123(92)90008-Z
8. Shi Y and Han Z. Effect of weld thermal cycle on microstructure and fracture toughness of simulated heat-affected zone for a 800 MPa grade high strength low alloy steel. *Journal of Materials Processing Technology*. 2008; 207(1-3):30-39. http://dx.doi.org/10.1016/j.jmatprotec.2007.12.049
9. Salazar-Garrido JA,Teran-Guillen J, García-Cerecero G, Martínez-Madrid M and Vargas-Arista B. Metallurgical Characterization of Grain Growth on Weldment by SMAW Process for a Steel AISI 4140. In: *Proceedings of the 30th Congreso Internacional de Metalurgia y Materiales*; 2008; Saltillo, México. Saltillo: Instituto Tecnológico de Saltillo; 2008. p. 97-105.
10. Qiu H, Mori H, Enoki M and Kishi T. Fracture Mechanism and Toughness of the Welding Heat-Affected Zone in Structural Steel under Static and Dynamic Loading. *Metallurgical and Materials Transactions A*. 2000; 31A(11):2785-2791.
11. Magudeeswaran G, Balasubramanian V and Madhusudhan RG. Effect of welding consumables on fatigue performance of shielded metal arc welded high strength, Q&T steel joints. *Journal of Materials Engineering and Performance*. 2009; 18(1):49-56. http://dx.doi.org/10.1007/s11665-008-9253-1
12. American Welding Society – AWS. *Standard D1.1*: Structural Welding Code Steel. 20th ed. Miami: American Welding Society; 2006. p. 57-61.
13. Chandler H. *Heat treater's guide*: practices and procedures for irons and steels. 2nd ed. ASM International; 2010. p. 319-325.
14. American Welding Society – AWS. *Specification A5.5*: Specification for low-alloy steel electrodes for shielded metal arc welding. Miami: American Welding Society; 2005. p. 1-68.
15. Ravi S, Balasubramanian V and Nemmat NS. Effect of Notch Location on Fatigue Crack Growth Behavior of Strength-Mismatched High-Strength Low-Alloy Steel Weldments. *Journal of Materials Engineering and Performance*. 2004; 13(6):758-765. http://dx.doi.org/10.1361/10599490420566
16. American Society for Testing and Materials – ASTM. *Standard E-399*: Standard test method for lineal-elastic plane-strain fracture toughness K_{IC} of metallic materials. West Conshohocken: ASTM; 2005. p. 15-17.
17. Kusko SC, Dupont NJ and Marder RA. The influence of microstructure on fatigue crack propagation behavior of stainless steel welds. *Welding Journal*. 2004; (1):6-14.